Journal of Zhejiang University-SCIENCE A (Applied Physics & Engineering) 2022 23(1):14-26
www.jzus.zju.edu.cn; www.springer.com/journal/11582
E-mail: jzus_a@zju.edu.cn

Research Article

https://doi.org/10.1631/jzus.A2100280

Check for updates

A biomimetic robot crawling bidirectionally with load inspired by rock-climbing fish

Jin-rong WANG[1], Yong-xin XI[2], Chen JI[3], Jun ZOU[1]✉

[1]*State Key Laboratory of Fluid Power and Mechatronic Systems, Zhejiang University, Hangzhou 310027, China*
[2]*College of Electrical Engineering, Zhejiang University, Hangzhou 310027, China*
[3]*Institute of Marine Science and Technology, Shandong University, Qingdao 266237, China*

Abstract: Using a unique adhesive locomotion system, the rock-climbing fish (*Beaufortia kweichowensis*) adheres to submerged surfaces and crawls both forwards and backwards in torrential streams. To emulate this mechanism, we present a biomimetic robot inspired by the locomotion model of the rock-climbing fish. The prototype contains two anisotropic adhesive components with linkages connected to a linear actuator. Each anisotropic adhesive component consists of one commercial sucker and two retractable bioinspired fin components. The fin components mimic the abduction and adduction of pectoral and pelvic fins through the retractable part to move up and down. The robot prototype was tested on vertical and inverted surfaces, and worked successfully. These results demonstrate that this novel system represents a new locomotion solution for surface movement without detachment from the substrate.

Key words: Fish kinematics; Adhesive locomotion mechanism; Fin rays motion; Climbing model; Bio-inspired robot

1 Introduction

In the transition from aquatic to terrestrial environments, some fish are able to walk underwater or on land using their pectoral fins and/or pelvic fins. For example, the mangrove rivulus (*Kryptolebias marmoratus*) uses a diverse suite of behaviors such as launches, squiggles, and pounces to move from water to land. The pectoral fins are used as pivot points to push and lift their bodies while they sweep their tails and heads through an S-shaped bend until they reach the opposite curvature in squiggles (Pronko et al., 2013). Lungfish (*Protopterus annectens*) use paired fins against a solid substrate for benthic locomotion, with gaits that range from walking to bounding, and pectoral fins play a major role in the propulsion (King et al., 2011). Mudskippers (*Periophthalmus variabilis*) are able to mechanically push their pelvic fins downward as their pectoral fins retract, allowing for an instant movement of pelvic fins during the pectoral fin backward stroke (Kawano and Blob, 2013; Wicaksono et al., 2018). Walking catfish (*Clarias anguillaris*) use their tails to push their bodies forward, pivoting over their pectoral fins. Cavefish (*Cryptotora thamicola*) use a diagonal-couplet lateral sequence gait, accomplished by rotation of their pectoral and pelvic girdles (Flammang et al., 2016). Freshwater eels (*Anguilla rostrate*) use their axial musculoskeletal system to move in an undulatory way. Similarly, some gobies (juvenile *Awaous guamensis*) climb waterfalls using powerful bursts of eel-like axial undulations initiated by pectoral fin adduction (Schoenfuss and Blob, 2003; Blob et al., 2007). Other fish have evolved adhesive apparatuses, which act like suckers (Ditsche et al., 2014). Some gobies (*Sicyopterus stimpsoni*) (Blob et al., 2007) and climbing catfish (*Astroblepidae, Siluriformes*) (de Crop et al., 2013) use oral and pelvic suckers to climb surfaces without axial undulation ("inching up"). Rock-climbing fish (*Beaufortia kweichowensis*) are extraordinary fish able to climb in fast-flowing currents. They have evolved adhesive suckers, enabling them to adhere to wet and slippery rocks and hold themselves in position (Zou et al.,

✉ Jun ZOU, junzou@zju.edu.cn
Jin-rong WANG, https://orcid.org/0000-0002-1963-1764

Received June 15, 2021; Revision accepted Aug. 6, 2021;
Crosschecked Oct. 26, 2021

© Zhejiang University Press 2022

2016). The fish crawl bidirectionally, controlled by retractable fins without detachment, and their girdle muscles instead of tails provide power in crawling (Wang et al., 2019). Unlike the rock-climbing fish, none of the previously mentioned fish, such as lungfish, mudskippers, and cavefish, walk with continuous contact with the substrate, because they need to lift up their fins. In locomotion, the tails are also used by some fishes like the mangrove rivulus and walking catfish. Gobies and climbing catfish use two suckers to work in an alternating pattern. However, sucker detachment has not been observed in the crawling of the rock-climbing fish. The locomotion mechanism of rock-climbing fish seems different from that of the previously mentioned fish, and climbing in an adhesive mode without detachment may be a more efficient and energy saving process during wall surface movement.

Biologically inspired robots showcase impressive locomotion characteristics. People are impressed by their numerous potential applications, which include inspection, diagnosis, and maintenance of buildings such as skyscrapers, drilling platforms, and nuclear storage plants. Bioinspired robots mean that we translate fundamental biological principles into engineering design rules to create robots that perform like natural systems. In recent years, many biomimetic robots have been proposed. Flying robots mimic the ability of pigeons or bats that are able to fly in the sky by morphing wings (Ijspeert, 2014; Chang et al., 2020). Swimming robots mimic the ability of squids and jellyfish that are able to swim in the water by pulse-jet propulsion (Xu and Dabiri, 2020; Bujard et al., 2021). Previous climbing robots generally employ three main adhesion methods: suction cups, adhesives, and magnets. Considering that most natural surfaces and some manmade surfaces such as concrete and brick exterior surfaces are rough and dusty, these adhesion methods are not generally suitable. In recent years, inspired by climbing animals, some novel adhesion methods have been developed. Climbing robots mimic the ability of gecko lizards that are able to climb up vertical surfaces by hierarchical structures (Kim et al., 2008; Kwak et al., 2011). Inspired by some insects and arthropods which can climb well on rough vertical surfaces using claws and miniature spines on the distal surfaces of their legs, climbing robots using miniature spines can climb rough and dusty vertical surfaces (Asbeck et al., 2006; Haynes et al., 2009). The major issues in the design of climbing robots relate to their locomotion and adhesive abilities. A reliable adhesion method would ensure that climbing robots would not fall off with sufficient payloads. A proper locomotion means that climbing robots can move under different circumstances, moving from horizontal surfaces to vertical surfaces. Stable adhesion and easy detachment (efficient locomotion) are not easy to achieve simultaneously in artificial systems. However, in nature animals have evolved this ability by directional adhesion structures through soft setae and rigid spines. The artificial structures inspired by animals are in micro or nano scale, which makes them difficult to fabricate and prone to wear. In rock-climbing fish adhesion, a mixture of gas and liquid fills the gap between the fish and the surface, so the fish is not in direct contact with the surface. The mixture of gas and liquid is easily renewable. During bidirectional crawling, detachment does not occur in rock-climbing fish, but adhesion and detachment appear repeatedly in gecko, insects, and related inspired robots. The adhesive locomotion mechanism without detachment in rock-climbing fish may solve the conflict between stable adhesion and efficient locomotion. This mechanism could be applied to robots to help them move on a large range of continuous surfaces with small obstacles, such as ship hulls, wind turbine blades, and oil tanks.

In this paper, we present a biomimetic robot inspired by the locomotion model of the rock-climbing fish. Firstly, a virtual prototype robot was built in SolidWorks. Secondly, the appropriate size of the robot was determined by parametric modeling. Then the components such as suckers, motors, and controllers were chosen by tests or calculations. The robot frame was fabricated by 3D printing technology. Finally, in tests, the robot was able to climb on vertical surfaces, and on an inverted surface carrying a load of 1000 g in addition to its own weight of 147 g. This research provides ideas and demonstrates the potential for the development of more efficient and loadable systems of wall surface movement in biomimetic robots.

2 Methods

2.1 Crawling locomotion modeling

According to our hypothesis in previous studies (Wang et al., 2019), we aimed to emulate the fish's

locomotion mechanism. First, a simplified locomotion model was defined (Fig. 1). The bilateral pectoral fins and chest comprise one unit called the anterior adhesive unit, and the bilateral ventral fins and abdomen comprise another unit called the posterior adhesive unit. The tiny movement of the tail was ignored in this locomotion modeling. The anterior and posterior adhesive units both contain a sucker and two lateral alterable friction modules mimicking the abduction and adduction of the fins. The girdle muscles function like extensible cylinders (Fig. 2).

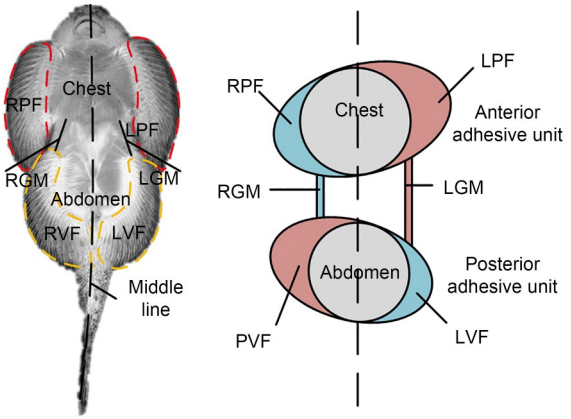

Fig. 1 Simplified model of the ventral view of *Beaufortia kweichowensis*. LPF: left pectoral fin; RPF: right pectoral fin; LVF: left ventral fin; RVF: right ventral fin; LGM: left girdle muscle; RGM: right girdle muscle. The abducted LPF is colored red, and the adducted RPF is colored blue. The protractor ischia of the LGM is colored red, and the retractor ischia of the RGM is colored blue (Note: for interpretation of the references to color in this figure, the reader is referred to the web version of this article)

2.2 Biomimetic robot modeling

The bio-robot has a design structure similar to that of a rock-climbing fish body. Identical anterior and posterior adhesive units are connected to a base frame through rotatable joints. An adhesive unit contains a sucker and two alterable friction modules. The alterable friction module realizes the function of different friction forces, like bilateral retractable fins. The alterable friction module has two states: high friction force and low friction force. These correspond to the abduction and adduction of pectoral and ventral fins, respectively (Fig. 3). During locomotion, the adhesive units rotate under some constraints. The biomimetic robot always adheres to the surface by two suckers, without sucker detachment. The diagonal alterable friction modules keep the same state at the same time, but the symmetric

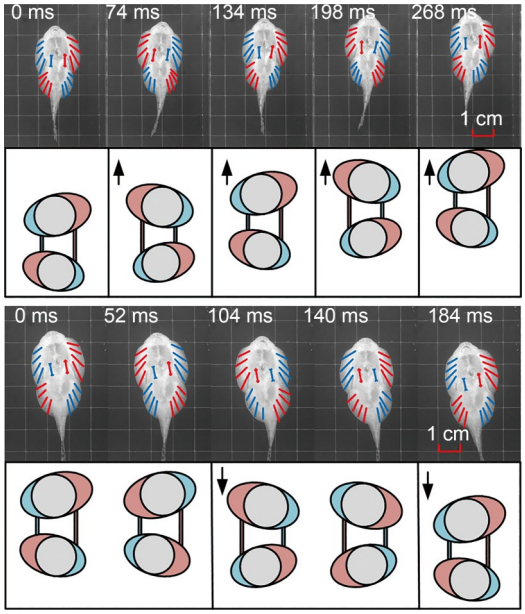

Fig. 2 Crawling locomotion modeling. Forward crawling and corresponding simplified schematic diagram (upper); backward crawling and corresponding simplified schematic diagram (lower). Red lines indicate abducted fin rays, and blue lines indicate adducted fin rays (Note: for interpretation of the references to color in this figure, the reader is referred to the web version of this article)

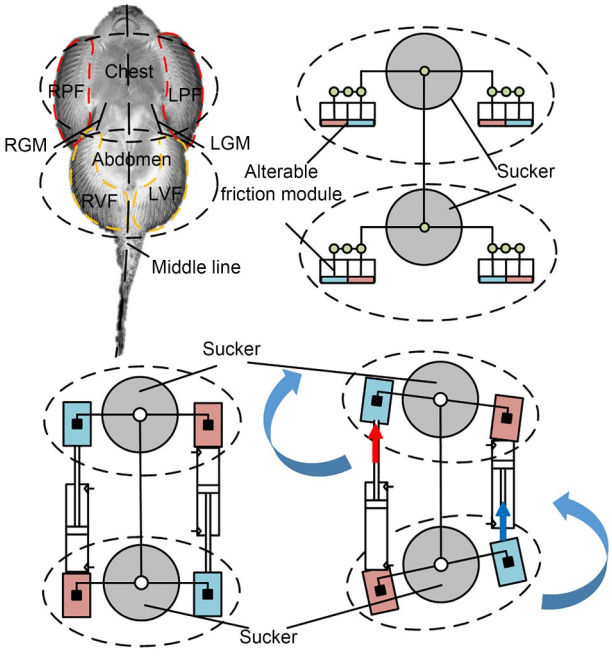

Fig. 3 Biomimetic robot model diagram. The adhesive unit in the chest of the fish corresponds to the anterior adhesive unit of the model, and the adhesive unit in the abdomen of the fish corresponds to the posterior adhesive unit of the model. Alterable friction modules in a high friction state are colored red, and those in a low friction state are colored blue (Note: for interpretation of the references to color in this figure, the reader is referred to the web version of this article)

alterable friction modules function differently. They all switch in cycles. The alterable friction module has a high friction force like unfolded fins, and a low friction force like folded fins. When activating two actuators, such as one extending and another retracting, the alterable friction module in low friction state will rotate around the module in high friction state in an adhesive unit. During this period, the biomimetic robot swings to one side just like a rock-climbing fish. As the cycle continues, the robot moves continuously.

2.2.1 Design of drive mode

Bilateral scalable actuators like girdle muscle always act in opposition, so a linkage drive mode was applied. To keep the features of light weight and easy control, a two bilateral actuator drive mode was not adopted. An actuator connecting linkage mechanism was adopted instead. Through the drive way of the lead screw slider, the slider connecting the linkage is pushed to move left and right, and the anterior and posterior adhesive units realize the swing effect around the robot axis (Fig. 4).

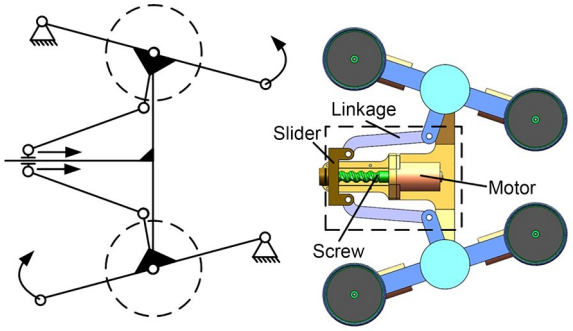

Fig. 4 Model of the drive mode and mechanism of the biomimetic robot. The drive mode contains a motor, screw, slider, and linkages in the dashed box

2.2.2 Design of adhesive unit

The adhesive unit contains two alterable friction modules which work in opposition. The stepping motors drive the cams to rotate periodically, and the cams drive the cam-followers to reciprocate up and down under the action of springs. The cam-follower, scaleboard, and friction plate in an alterable friction module are rigidly connected (Fig. 5). When the rotating cam makes the cam-follower move to the lower limit position, the friction plate is completely pushed out from the sleeve, and in contact with the surface. The cam continues to rotate, and the cam-follower is

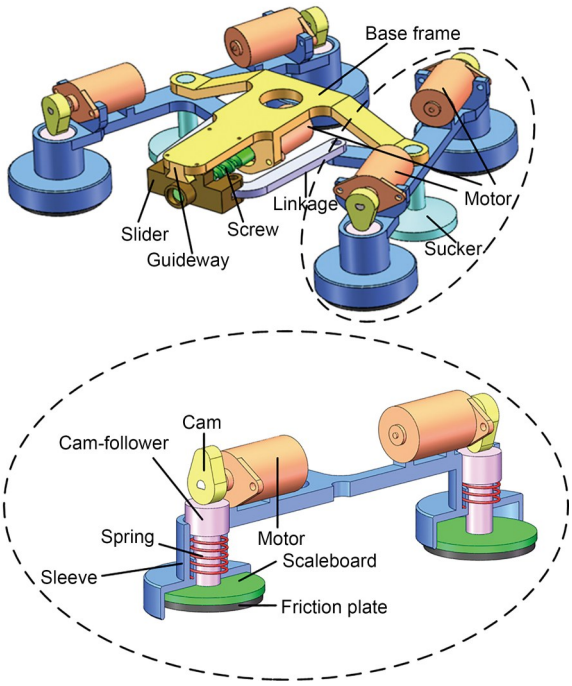

Fig. 5 Biomimetic robot prototype including adhesive unit and alterable friction modules. The biomimetic robot virtual prototype has two adhesive units. Each adhesive unit (shown in the upper dashed oval) has one sucker and two alterable modules. The adhesive unit contains two alterable friction modules which are realized by a cam, cam-follower, and spring. This mechanical structure can move the friction plate up and down (lower dashed oval)

pushed to the upper limit position under the action of the spring. At this time, the friction plate is completely retracted in the sleeve and cannot contact the surface.

In this process, the friction plate is periodically up or down along the sleeve with the cam follower. When the friction plate is in contact with the surface, the alterable friction module of the adhesive unit is in a high friction state, which corresponds to the abduction state of the fins of the rock-climbing fish. The corresponding alterable friction module produces a large friction force with the surface when crawling. When the friction plate is withdrawn into the sleeve, the alterable friction module of the adhesive unit is in a low friction state, and the friction between the corresponding alterable friction module and the surface is small when crawling.

2.2.3 Parameter definition

According to the motion design principle of the biomimetic robot, in the process of motion, the suction cup is responsible for providing the adhesion force of

the robot to the surface, so the robot will continue to adhere to the surface. The alterable friction module provides additional friction between the robot and the surface. In addition to promoting swing motion, it prevents the robot from sliding on the surface. The swing drive module acts as an actuator of the biomimetic robot.

The structural parameters need to be optimized and determined in the design, so the relevant parameters of the biomimetic robot should be defined (Fig. 6).

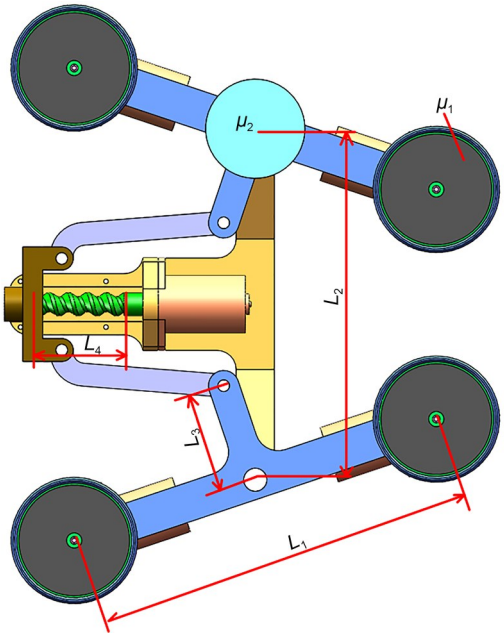

Fig. 6 Parameter definition of the biomimetic robot. The distance between two alterable friction modules in an adhesive unit is defined as L_1; the distance between two adhesive units is defined as L_2; the linkage length between the sucker and the connection with the drive unit is defined as L_3; the effective length of the slider is L_4; the friction coefficient between the friction plate and acrylic plate is μ_1; the friction coefficient between the sucker and the polymethyl methacrylate (PMMA) substrate is μ_2

2.2.4 Parameter determination

In the selection of the sucker, two aspects should be considered. On the one hand, the sucker needs to provide enough adhesion force to ensure that the biomimetic robot does not fall from the surface. On the other hand, the friction coefficient between the sucker and the surface should be as small as possible to reduce the obstruction of the sucker to movement. To determine the specific parameters of the sucker used in the biomimetic robot, the relative static and dynamic friction coefficients of common vacuum suckers and the adhesion force generated under the same tensile height were measured (Fig. 7).

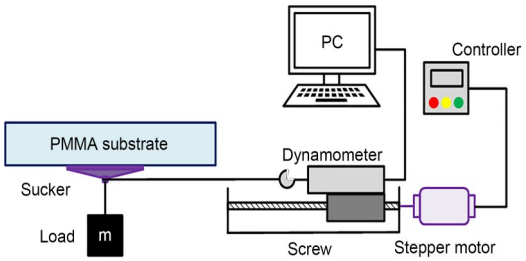

Fig. 7 Setup for measuring the friction coefficient of different suckers. The sucker is adhered to the PMMA bottom surface, then a load is hung on the sucker. The stepper motor drives the screw to rotate after turning on the controller, and the dynamometer pulls the sucker to slip in a horizontal direction by means of a nylon thread

The suckers tested in the sucker selection experiment included: silicone rubber ribbed suckers (diameters of 20, 25, 32, and 40 mm), common silicone rubber suckers (diameters of 20, 25, 32, and 40 mm), nitrile rubber ribbed suckers (diameters of 20, 25, 32, and 40 mm), and common nitrile rubber suckers (diameters of 20, 25, 32, and 40 mm). The surface material was acrylic. The connection of the sucker to the vacuum equipment was sealed with rubber solution. Following friction coefficient tests of four kinds of suckers and the PMMA substrate with a total of 16 specifications, the nitrile suckers were found to be stiffer and more adhesive than silicone suckers, and less likely to slip in the horizontal direction. The common suckers without ribs were easily deformed, and the deformation causes failure in adhesion. The friction of the suckers, except the silicone rubber ribbed suckers, was not tested in detail. The friction coefficient between the silicone rubber ribbed suckers and the PMMA substrate was relatively small. The static friction coefficient was about 3.15, and the dynamic friction coefficient was about 2.10, much less than those of other kinds of suckers. Next, the adhesion force generated by the sucker being pulled up by 2 mm in the adhesive state was measured. The adhesion forces generated by the silicone rubber ribbed suckers with diameters of 20, 25, 32, and 40 mm were about 2.10, 4.50, 6.0, and 10.4 N, respectively. Considering the friction coefficient and adhesion force of the four kinds of suckers with 16 specifications, the silicone rubber ribbed sucker with a diameter of 32 mm was selected as the sucker for the biomimetic robot.

In a cycle of the biomimetic robot's crawling process, the adhesive units will rotate at a certain angle around the left alterable friction module or the right alterable friction module. The movement trajectory of the posterior adhesive unit in a movement cycle is shown in Fig. 8. The axial displacement length of the biomimetic robot in one cycle is L_X.

$$L_X = 2 \times L_1 \sin \frac{\alpha}{2}. \tag{1}$$

When the biomimetic robot's posterior adhesive unit rotates from one limit position to another, the rotation angle α is exactly the same as the angle β. When the connecting rod in the frame rotates from the right limit position to the left limit position, the radial displacement moved by the end of the connecting linkage is the effective movement range length L_4 of the threaded slider.

$$\beta = 2 \times \arcsin \frac{L_4}{2 \times L_3}, \tag{2}$$

$$\text{and } \alpha = \beta, \tag{3}$$

$$\text{then } L_X = \frac{L_1 \times L_4}{L_3}. \tag{4}$$

The displacement of the biomimetic robot in the axial direction is positively correlated with the distance L_1 (the length between two alterable friction modules in an adhesive unit) and the length L_4 (the effective motion range of the threaded slider), and negatively correlated with the length L_3 (the length of the linkage in Fig. 8).

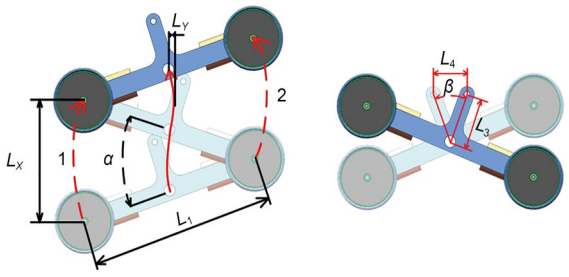

Fig. 8 Displacement trajectory and relationship in a cycle. The solid curve shows the displacement curve of the suction cup of the adhesive unit in the posterior of the biomimetic robot in one cycle. That is also the displacement curve of the biomimetic robot in a cycle. The dashed curves show the displacement curve of the alterable friction module of the adhesive unit in the posterior of the biomimetic robot in half a cycle

The displacement of the biomimetic robot in the radial direction is periodic, and the displacement curve of the biomimetic robot in a cycle is two symmetrical arcs. The amplitude of the left-right swing in a cycle, L_Y is:

$$L_Y = \frac{L_1}{2} - \frac{L_1}{2} \times \cos \frac{\alpha}{2}. \tag{5}$$

In the screw-slider drive module of the biomimetic robot, the stepper motor drives the screw to rotate periodically and then pushes the slider to move along the linear guideway. Assuming that the pitch of the screw is p (single helical line), the speed of the stepper motor in the screw-slider drive module is n_1:

$$n_1 = \frac{L_4}{p \times t}, \tag{6}$$

where t is the time required for the slider to move the length of L_4.

A rock-climbing fish is generally about 50 mm× 50 mm×20 mm (Zou et al., 2016). In consideration of the limitation of part sizes, in the process of biomimetic robot research and production, the length, width, and height of the biomimetic robot were limited to about 100 mm, 100 mm, and 40 mm, respectively. The axial displacement of one cycle in real fish is about 5 mm, which is about 10% of the fish's total length. During crawling, the length of girdle muscle varies by 2 mm (Wang et al., 2019), and this is a small distance for common 3D printing parts and actuators with low precision. To increase the displacement of the robot in a cycle and to facilitate fabrication, the axial displacement in a cycle was about 50 to 100 mm, which is between half and one total length of the robot. The cycle time was about 6 s for an appropriate observation with a common digital camera and the human eye. According to the three requirements, the biomimetic robot parameters were broadly determined. L_1 was set as 100 mm. The installation of the suckers in the biomimetic robot and the installation size of the robot base frame were taken into account to avoid installation interference. L_3 was set as 25 mm.

The axial displacement is required to be between 50 and 100 mm within a movement cycle, the distance L_1 between the two alterable friction modules was defined as 100 mm, and the length L_3 of the

connecting linkage was 25 mm. We concluded that the effective motion range length L_4 of the thread slider was 12.5 to 25 mm. According to Eq. (6), the greater the value of the effective motion range L_4 of the threaded slider, the faster the motor speed required, and the faster the motor speed, the lower the torque that the motor can provide. After taking the above two factors into consideration, the effective motion range L_4 length of the slider was set as 15 mm, and the pitch of the screw as 5 mm. Therefore, when the slider moves from the left limit position to the right limit position once, the stepping motor needs to rotate three laps. β is calculated from Eq. (2) as 34.9°. L_2 was set as 90 mm directly. If the diameter is too small, the friction of the biomimetic robot declines. If the diameter is too large, the alterable friction module interferes with the rest of the frame, and the weight of the biomimetic robot increases. Therefore, after thorough consideration of the above aspects, the diameter of the friction plate was set as 28 mm, and the overall diameter of the alterable friction module as 31 mm.

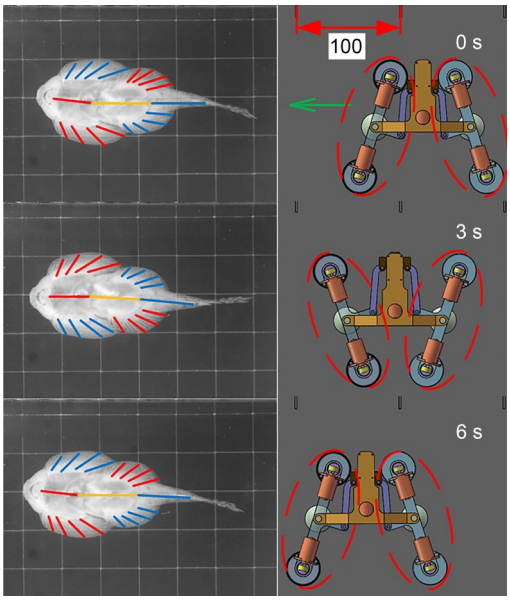

Fig. 9 A locomotion cycle of the biomimetic robot. The body line is divided into three parts with different colors (red, yellow, and blue). The red line indicates the mid-pectoral line, the yellow line indicates the mid-ventral line, and the blue line indicates the mid-tail line. Red lines mean abducted and blue lines mean adducted fin rays (Note: for interpretation of the references to color in this figure, the reader is referred to the web version of this article)

3 Results

3.1 Biological similarity in locomotion

The virtual prototype of a rock-climbing fish biomimetic robot was simulated using SolidWorks Motion. Fig. 9 shows the gait of the robot at 0, 3, and 6 s within a locomotion cycle. In SolidWorks motion, the trace point is set in the center of the sucker in the anterior adhesive unit during a locomotion cycle. Fig. 10 shows the movement track of the posterior sucker in one cycle, that is, the movement track of the robot in one cycle. In high speed recording and point tracing technology of real fish, the trace point is set in the center of the sucker in the headmost point of the fish head during a locomotion cycle. Details of the method can be found in (Wang et al., 2019). Fig. 11 shows the trajectory of a rock-climbing fish during multiple swing processes as it moves forward. Comparing Figs. 10 and 11 shows that the movement trajectories of the robot and fish are similar, both with trajectories zigzagging and swinging forward.

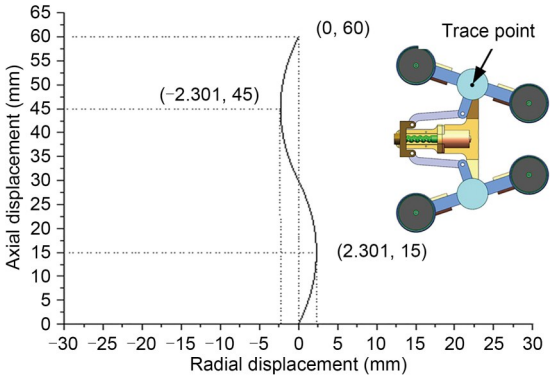

Fig. 10 Movement trajectory in a cycle of the robot. This figure was obtained using SolidWorks motion. The trace point is in the center of the sucker in the anterior adhesive unit during a locomotion cycle

3.2 Mechanical structure

The fabrication of the mechanical system of the biomimetic robot includes mainly the processing and assembly of each mechanism's linkages, the fabrication of the friction plates in the alterable friction modules, and the selection of the stepper motor. All the linkages in the biomimetic robot model can be directly produced by 3D printing. The material used was Future Resin 8000, a commonly used 3D printing material.

The suckers of the biomimetic robot are silicone rubber ribbed suckers. The static friction coefficient between the sucker and the surface is about 3.15, and

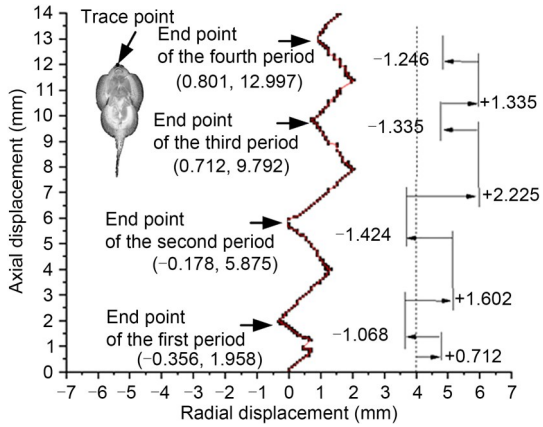

Fig. 11 Movement trajectory in four cycles of the fish. This figure was obtained by high speed recording and point tracing technology of real fish. The trace point is in the headmost point of the fish head during a locomotion cycle

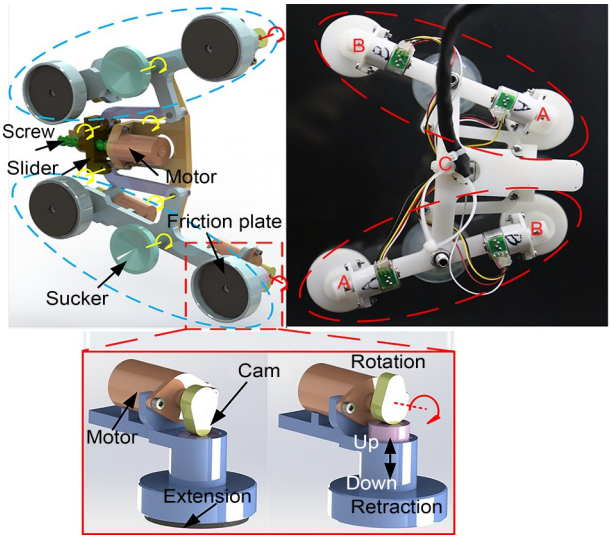

Fig. 12 Mechanical system of the biomimetic robot (the virtual robot prototype in SolidWorks). The yellow curves with an arrow denote the rotatable joints in the linkages, and the red curves with an arrow denote the rotatable cams (Note: for interpretation of the references to color in this figure, the reader is referred to the web version of this article)

the dynamic friction coefficient is about 2.10. According to the SolidWorks Motion simulation results, the friction coefficient of the friction plate should be greater than 1.8 times that of the suction cup, and the greater the friction coefficient, the more conducive it is to the robot's crawling within the allowable power range of the stepping motor.

In the fabrication of the friction plate, silicone gel was directly poured into the friction plate mold. Several gels of different hardness were poured into the friction plate and the friction coefficient on the surface of the acrylic plate was tested. After a series of tests, a silicone gel with a hardness of 0030 was selected to make the friction plate. The coefficient of static friction between the friction plate and the surface was 7.25, which is 2.3 times the static friction coefficient of the sucker. The coefficient of dynamic friction between the friction plate and the surface was 4.6, which is 2.19 times the dynamic friction coefficient of the sucker.

According to the simulation results, the peak output torque of the motors of the alterable friction modules is 12.693 N·mm when the speed is 75 r/min, and the safety factor was set as 1.5 here. Therefore, when the speed is 75 r/min, the rated output torque of the stepper motor should be 19.04 N·mm. Because the output torque of the motor for the screw-slider has no actual reference value for when the stepper motor rotation speed is 101 r/min, the required output rated torque was based on robot locomotion experiments. Here, all motors were the same as the stepper motors (GM12-15BY) (Fig. 12).

3.3 Control system

The control system involves the remote control operation and control of the five stepper motors in accordance with the specified law of rotation. To realize the drive control of the stepper motor, it is necessary to select the driver and controller. To realize remote control functions, a corresponding wireless remote module is needed.

The selected stepper motors were two-phase four-wire systems, with a rated voltage of 5–12 V, and a no load rated current of 0.15 A. The relevant supporting requirements of the stepper motor and the weight of the whole control system were considered. The driver model chosen was TB6560. The selected wireless remote module was APDC-6K (Anping six wireless remote control). The chosen controller was an Arduino UNO R3 (Fig. 13).

3.4 Crawling test of the biomimetic robot

The engineering prototype of the biomimetic robot was tested on a variety of surfaces, such as horizontal, vertical, and inverted planes. Crawling on these surfaces was completed successfully. We also tested crawling with a load on an inverted surface.

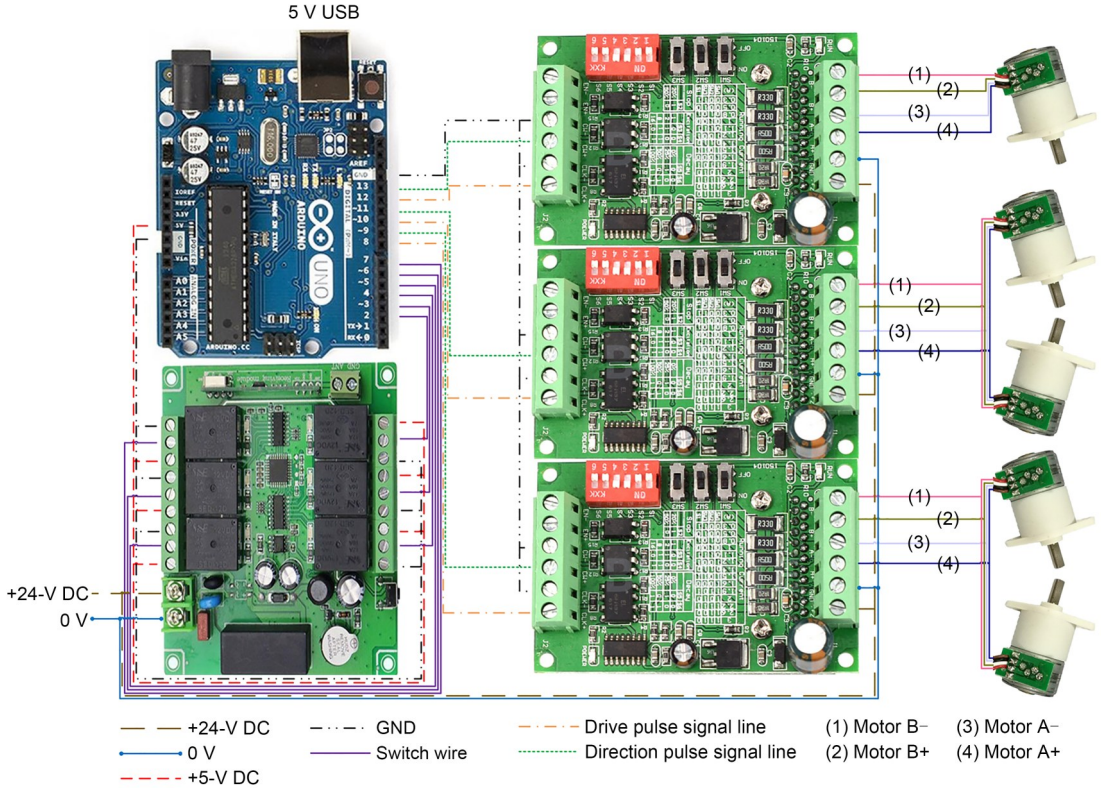

Fig. 13 Control circuit diagram. USB: universal serial bus; GND: ground

3.4.1 Crawling on a horizontal plane

When the robot crawls on a horizontal surface, the suction cups provide the minimum adhesion force to reduce the friction moment caused by the suction cups as much as possible. Gravity is offset by the positive pressure of the alterable friction modules and the suckers, so it is easier to crawl.

Fig. 14 shows the recoding of horizontal surface crawling, and Fig. 15 shows the adhesive crawling of the robot on the horizontal surface. The movement process of the horizontal surface crawling experiment was as follows:

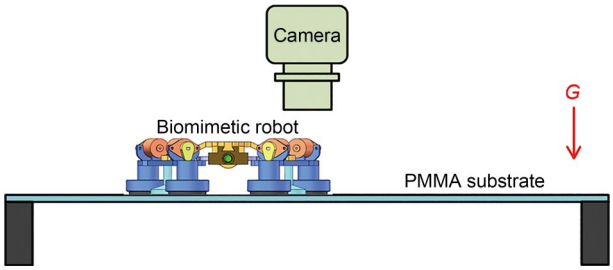

Fig. 14 Recoding schematic diagram of crawling on a horizontal surface. The lens of the camera points to the top of the robot which is on the PMMA substrate. *G* means gravity

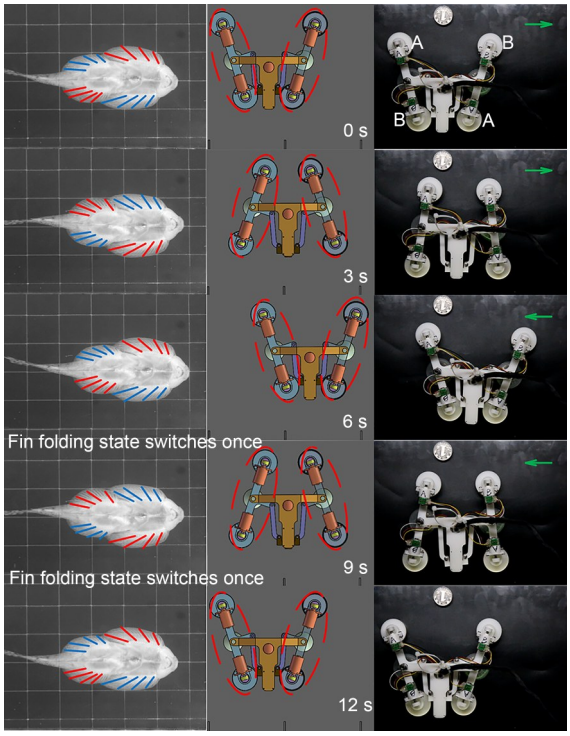

Fig. 15 Crawling on a horizontal plane. The left column shows the real fish, the middle column shows the virtual robot prototype in SolidWorks Motion, and the right column shows the actual robot

(1) Forward status (0–3 s)

The fin-like alterable friction modules of group A are lifted and the thread slider pushed out. Theanterior and posterior adhesive units are driven to twist with the fin-like alterable friction modules of group B as the center to complete the first half cycle movement in the forward state.

(2) Forward state (3–6 s)

The fin-like alterable friction modules of group B are lifted and the thread slider pulled back. The anterior and posterior adhesive units are driven to twist with the fin-like alterable friction modules of group A as the center to complete the second half cycle movement in the forward state.

(3) Backward state (6–9 s)

The fin-like alterable friction modules of group B are lifted and the thread slider pushed out. The anterior and posterior adhesive units are driven to twist with the fin-like alterable friction modules of group A as the center to complete the first half cycle movement in the backward state.

(4) Backward state (9–12 s)

The fin-like alterable friction modules of group A are lifted and the thread slider pulled back. The anterior and posterior adhesive units are driven to twist around the fin-like alterable friction modules of group B to complete the second half cycle movement in the backward state.

The duration of one complete forward or backward cycle was 6 s. This test contained both forward and backward cycles, so the whole test time was 12 s. One CNY coin was taken as a reference, and data were processed by ImageJ. In forward crawling, the first movement in 2 s was about 20.16 mm, and the speed about 10.08 mm/s. The second movement in 2 s was about 20.98 mm, and the speed about 10.49 mm/s. In backward crawling, the first movement in 2 s was about 24.00 mm, and the speed about 12.00 mm/s. The second movement in 2 s was about 22.02 mm, and the speed about 11.01 mm/s.

3.4.2 Crawling on a vertical wall

When the biomimetic robot crawls on a vertical surface wall, its own gravity is overcome by group A and group B fin-like alterable friction modules and the friction between the two suckers and the wall. The magnitude of the friction depends on the initial adhesion force between the suckers and the wall. Compared with the horizontal surface, the vertical wall is more difficult to climb.

Fig. 16 shows the recoding of vertical wall surface crawling, and Fig. 17 shows the adhesive crawling motion of the robot on the vertical wall surface. The movement process of the robot in the vertical wall crawling experiment is consistent with that in the horizontal wall crawling experiment.

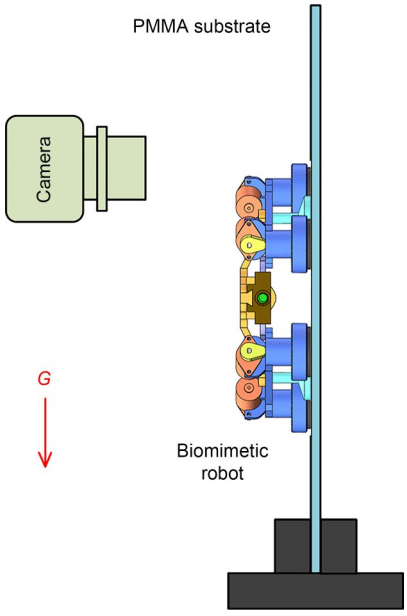

Fig. 16 Recoding schematic diagram of crawling on a vertical surface. The lens of the camera points to the top of the robot which is on the PMMA substrate

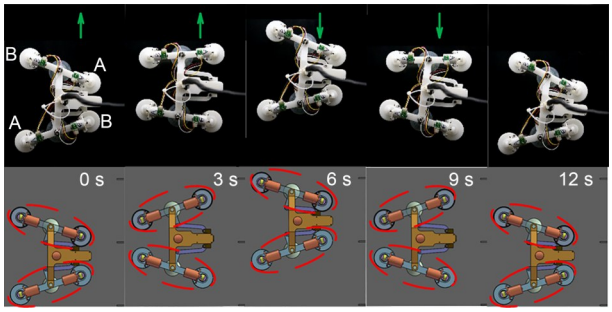

Fig. 17 Crawling on a vertical surface. The upper row shows the actual robot, and the lower row shows the virtual robot prototype in SolidWorks Motion

3.4.3 Crawling on an inverted plane

When the biomimetic robot is adhering and crawling on an inverted surface, its own gravity is completely offset by the adhesion force of the suction cups. The friction between the fin-like alterable friction modules in group A and group B and the surface

makes the robot move forward and backward. Therefore, adhering and crawling is easier on an inverted surface than on a vertical surface. Fig. 18 shows recoding of inverted surface crawling, and Fig. 19 shows the adhesive crawling motion of the robot on the inverted surface. The movement process of the robot in the inverted surface crawling experiment is consistent with that in the horizontal wall crawling experiment.

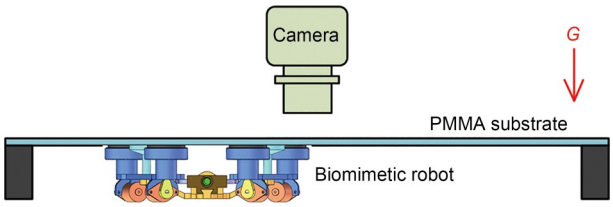

Fig. 18 Recoding schematic diagram of crawling on an inverted surface. The lens of the camera points to the bottom of the robot which is on the PMMA substrate

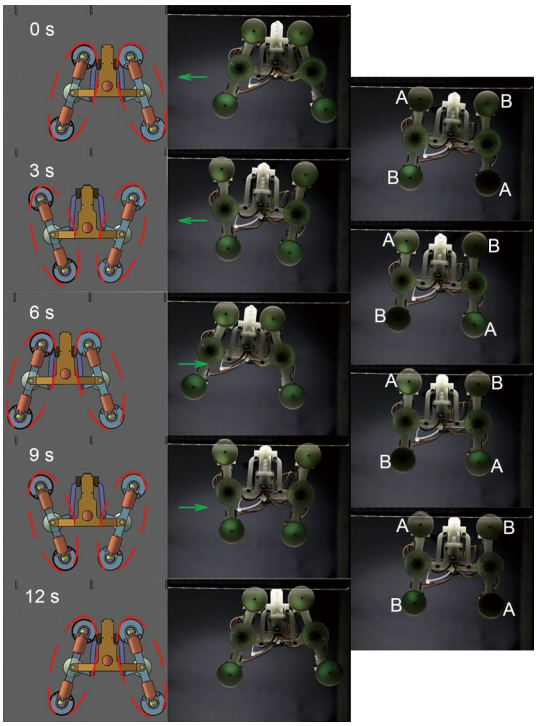

Fig. 19 Crawling on an inverted surface. The left column shows the virtual robot prototype in SolidWorks Motion. The middle column shows the final state of the actual robot in every half forward or backward cycle of motion. The right column shows the intermediate motion state of the actual robot. Areas with green light spots denote areas of contact (Note: for interpretation of the references to color in this figure, the reader is referred to the web version of this article)

In addition, due to the phenomenon of frustrated total internal reflection (FTIR) (Castillo et al., 2006), green light flecks are produced when the sucker and friction plates of the fin-like alterable friction modules contact the surface. In Fig. 19, the middle column of pictures shows the final state of the robot in every half forward or backward cycle of motion. Two suckers and four groups of fin-like alterable friction modules are in complete contact with the surface, producing green light spots. The right column of pictures shows the intermediate motion state of the robot. Combined with the movement process of the adhering and crawling experiment, it can be seen that:

(1) Forward state (0–3 s)

The fin-like alterable friction modules in group A lift up, and then the fin-like alterable friction modules in group B contact the surface and produce green light spots.

(2) Forward state (3–6 s)

The fin-like alterable friction modules in group B lift up, and then the fin-like alterable friction modules in group A contact the surface and produce green light spots.

(3) Backward state (6–9 s)

The fin-like alterable friction modules in group B lift up again, and this time, the fin-like alterable friction modules in group A contact the surface and produce green light spots.

(4) Backward state (9–12 s)

The fin-like alterable friction modules in group A lift up, and the fin-like alterable friction modules in group B contact the surface and produce green light spots.

3.4.4 Crawling with a load on an inverted plane

When the biomimetic robot crawls on an inverted surface, the vertical forces are completely offset by the suction force of the suckers, so the robot can bear a certain weight. The loading capacity is completely dependent on the maximum adhesion force provided by the suckers, which is affected by their diameter. Under constant negative pressure, the larger the diameter of the sucker, the greater the adhesion force. In the robot made in this study, the diameter of the suction cup was limited by the scale of the whole device, so there was an upper limit for the robot to adhere and crawl on the inverted surface.

In this experiment, weights of 200, 400, 500, 750, 1000, and 1250 g were tested. When the weight reached 1250 g, the sucker of the robot failed in the

process of crawling. Therefore, we consider that the bearable load of the robot is less than 1250 g, but more than 1000 g. Fig. 20 shows the adhering and crawling condition of the robot when the load was 1000 g.

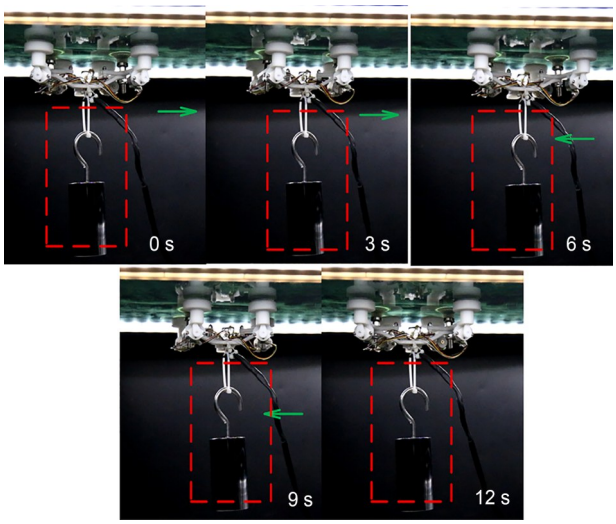

Fig. 20 Crawling with a load on an inverted surface. The weight of 1000 g is inside the dashed box

4 Conclusions

A unique system of locomotion based on an adhesive undulation mode was identified in rock-climbing fish. The locomotion system contains two anisotropic suckers associated with the pectoral and pelvic fins and two girdle muscles. During crawling, the states of the bilateral fins determine the direction of motion, and the bilateral girdle muscles provide power. Through a series of film recordings, this adhesive locomotion system was shown to be very effective on vertical or inverted surfaces, allowing the fish to move without detaching from the substrates. A biomimetic robot was fabricated just like the fish in locomotion, and a series of tests were carried out to show its locomotion features.

However, limited by progress in research of biomimetic suckers inspired by rock-climbing fish, high-performance biomimetic anisotropic adhesion is not currently realized. Ordinary commercial suckers without anisotropy were used in this study, and the adhesion tenacity of the robot was not high. So, the fabrication of bio-inspired suckers is the next research project, to solve the tenacity problem. A simple retractable mechanism was applied to realize different frictions, but there is a huge difference between the robot and the real fish in their manner of fin folding. A rigid frame was used in the robot here. Compared with the flexible spine of the fish, the robot lacks flexibility of movement perpendicular to the surface and cannot switch to a different surface at present. The goal of combining both form and function has not been achieved.

This biomimetic robot represents a loadable biomimetic solution to the problem of climbing while adhering to inclined surfaces. A new surface locomotion mode is proposed, which can be used in situations in which a single surface needs to be worked on for a long time. It reduces the demands for vacuum equipment to be carried, removes the need for a detachment stage, and solves the contradiction between adhesion and detachment.

Acknowledgments

This work is supported by the China Postdoctoral Science Foundation (No. 2020M681843), the National Natural Science Foundation of China (Nos. 51875507, 51821093, and 51890885), the Zhejiang Provincial Natural Science Foundation for Distinguished Young Scholars (No. LR15E050001), and the Zhejiang Provincial Natural Science Foundation of China (No. LY18E050003).

Author contributions

Jin-rong WANG, Yong-xin XI, Chen JI, and Jun ZOU designed the research. Jin-rong WANG performed the experiments and fabricated the robot. Jin-rong WANG wrote the first draft of the manuscript. Jin-rong WANG, Chen JI, and Jun ZOU revised and edited the final version.

Compliance with ethics guidelines

Jin-rong WANG, Yong-xin XI, Chen JI, and Jun ZOU declare that they have no conflict of interest.

All institutional and national guidelines for the care and use of laboratory animals were followed. The study was approved by Animal Welfare Committee of Zhejiang University, China (Authorization number: ZJU20170632).

References

Asbeck AT, Kim S, Cutkosky MR, et al., 2006. Scaling hard vertical surfaces with compliant microspine arrays. *The International Journal of Robotics Research*, 25(12): 1165-1179. https://doi.org/10.1177/0278364906072511

Blob RW, Wright KM, Becker M, et al., 2007. Ontogenetic change in novel functions: waterfall climbing in adult Hawaiian gobiid fishes. *Journal of Zoology*, 273(2):200-209. https://doi.org/10.1111/j.1469-7998.2007.00315.x

Bujard T, Giorgio-Serchi F, Weymouth GD, 2021. A resonant squid-inspired robot unlocks biological propulsive efficiency. *Science Robotics*, 6(50):eabd2971. https://doi.org/10.1126/scirobotics.abd2971

Castillo J, de la Blanca AP, Cabrera JA, et al., 2006. An optical tire contact pressure test bench. *Vehicle System Dynamics*, 44(3):207-221. https://doi.org/10.1080/00423110500171158

Chang E, Matloff LY, Stowers AK, et al., 2020. Soft biohybrid morphing wings with feathers underactuated by wrist and finger motion. *Science Robotics*, 5(38): eaay1246. https://doi.org/10.1126/scirobotics.aay1246

de Crop W, Pauwels E, van Hoorebeke L, et al., 2013. Functional morphology of the Andean climbing catfishes (*Astroblepidae, siluriformes*): alternative ways of respiration, adhesion, and locomotion using the mouth. *Journal of Morphology*, 274(10):1164-1179. https://doi.org/10.1002/jmor.20169

Ditsche P, Wainwright DK, Summers AP, 2014. Attachment to challenging substrates–fouling, roughness and limits of adhesion in the northern clingfish (*Gobiesox maeandricus*). *Journal of Experimental Biology*, 217(14):2548-2554. https://doi.org/10.1242/jeb.100149

Flammang BE, Suvarnaraksha A, Markiewicz J, et al., 2016. Tetrapod-like pelvic girdle in a walking cavefish. *Scientific Reports*, 6:23711. https://doi.org/10.1038/srep23711

Haynes GC, Khripin A, Lynch G, et al., 2009. Rapid pole climbing with a quadrupedal robot. Proceedings of the IEEE International Conference on Robotics and Automation, p.2767-2772. https://doi.org/10.1109/ROBOT. 2009.5152830

Ijspeert AJ, 2014. Biorobotics: using robots to emulate and investigate agile locomotion. *Science*, 346(6206):196-203. https://doi.org/10.1126/science.1254486

Kawano SM, Blob RW, 2013. Propulsive forces of mudskipper fins and salamander limbs during terrestrial locomotion: implications for the invasion of land. *Integrative and Comparative Biology*, 53(2):283-294. https://doi.org/10.1093/icb/ict051

Kim S, Spenko M, Trujillo S, et al., 2008. Smooth vertical surface climbing with directional adhesion. *IEEE Transactions on Robotics*, 24(1):65-74. https://doi.org/10.1109/TRO.2007.909786

King HM, Shubin NH, Coates MI, et al., 2011. Behavioral evidence for the evolution of walking and bounding before terrestriality in sarcopterygian fishes. *Proceedings of the National Academy of Sciences of the United States of America*, 108(52):21146-21151. https://doi.org/10.1073/pnas.1118669109

Kwak MK, Pang C, Jeong HE, et al., 2011. Towards the next level of bioinspired dry adhesives: new designs and applications. *Advanced Functional Materials*, 21(19): 3606-3616. https://doi.org/10.1002/adfm.201100982

Pronko AJ, Perlman BM, Ashley-Ross MA, 2013. Launches, squiggles and pounces, oh my! The water–land transition in mangrove rivulus (*Kryptolebias marmoratus*). *Journal of Experimental Biology*, 216(21):3988-3995. https://doi.org/10.1242/jeb.089961

Schoenfuss HL, Blob RW, 2003. Kinematics of waterfall climbing in Hawaiian freshwater fishes (*Gobiidae*): vertical propulsion at the aquatic–terrestrial interface. *Journal of Zoology*, 261(2):191-205. https://doi.org/10.1017/S0952836903004102

Wang JR, Ji C, Wang W, et al., 2019. An adhesive locomotion model for the rock-climbing fish, *Beaufortia kweichowensis*. *Scientific Reports*, 9(1):16571. https://doi.org/10.1038/s41598-019-53027-2

Wicaksono A, Hidayat S, Retnoaji B, et al., 2018. A mechanical piston action may assist pelvic-pectoral fin antagonism in tree-climbing fish. *Journal of the Marine Biological Association of the United Kingdom*, 98(8):2121-2131. https://doi.org/10.1017/S0025315417001722

Xu NW, Dabiri JO, 2020. Low-power microelectronics embedded in live jellyfish enhance propulsion. *Science Advance*, 6(5):eaaz3194. https://doi.org/10.1126/sciadv.aaz3194

Zou J, Wang JR, Ji C, 2016. The adhesive system and anisotropic shear force of Guizhou gastromyzontidae. *Scientific Reports*, 6:37221. https://doi.org/10.1038/srep37221